UCLA
UCLA Previously Published Works

Title

Leukemia Cell Cycle Chemical Profiling Identifies the G2-Phase Leukemia Specific Inhibitor Leusin-1

Permalink

https://escholarship.org/uc/item/16b370dx

Journal

ACS Chemical Biology, 14(5)

ISSN

1554-8929

Authors

Xia, Xiaoyu
Lo, Yu-Chen
Gholkar, Ankur A
et al.

Publication Date

2019-05-17

DOI

10.1021/acschembio.9b00173

Peer reviewed

Cite This: ACS Chem. Biol. XXXX, XXX, XXX–XXX

Articles

pubs.acs.org/acschemicalbiology

Leukemia Cell Cycle Chemical Profiling Identifies the G2-Phase Leukemia Specific Inhibitor Leusin-1

Xiaoyu Xia,[†] Yu-Chen Lo,[†,‡] Ankur A. Gholkar,[†] Silvia Senese,[†] Joseph Y. Ong,[†] Erick F. Velasquez,[†] Robert Damoiseaux,[§,∥] and Jorge Z. Torres*,[†,⊥,#] ⬤

[†]Department of Chemistry and Biochemistry, [‡]Program in Bioengineering, [§]Department of Molecular and Medical Pharmacology, [∥]California NanoSystems Institute, [⊥]Jonsson Comprehensive Cancer Center, and [#]Molecular Biology Institute, University of California, Los Angeles, California 90095, United States

Ⓢ Supporting Information

ABSTRACT: Targeting the leukemia proliferation cycle has been a successful approach to developing antileukemic therapies. However, drug screening efforts to identify novel antileukemic agents have been hampered by the lack of a suitable high-throughput screening platform for suspension cells that does not rely on flow-cytometry analyses. We report the development of a novel leukemia cell-based high-throughput chemical screening platform for the discovery of cell cycle phase specific inhibitors that utilizes chemical cell cycle profiling. We have used this approach to analyze the cell cycle response of acute lymphoblastic leukemia CCRF-CEM cells to each of 181420 druglike compounds. This approach yielded cell cycle phase specific inhibitors of leukemia cell proliferation. Further analyses of the top G2-phase and M-phase inhibitors identified the leukemia specific inhibitor 1 (Leusin-1). Leusin-1 arrests cells in G2 phase and triggers an apoptotic cell death. Most importantly, Leusin-1 was more active in acute lymphoblastic leukemia cells than other types of leukemias, non-blood cancers, or normal cells and represents a lead molecule for developing antileukemic drugs.
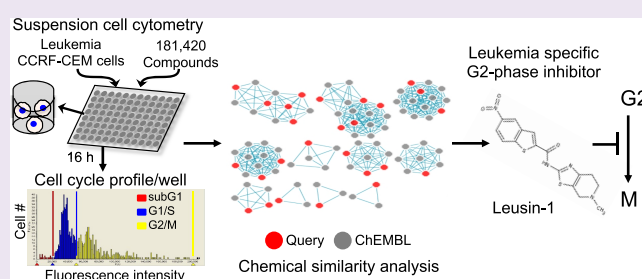
Acute lymphoblastic leukemia (ALL) originates from single B- or T-lymphocyte progenitors that proliferate and accumulate, resulting in the suppression of normal hematopoesis.[1] The disease is most common in children but can occur in any age group.[1] A successful strategy in the treatment of leukemias has been to inhibit leukemia cell proliferation by targeting DNA synthesis, protein synthesis, cell cycle progression, and proliferation-promoting signaling cascades.[1] Although some antileukemic drugs have been successful at treating specific types of leukemias, most have limited efficacies, mainly due to leukemia cell drug resistance mechanisms, a lack of specificity, and toxic side effects.[2−5] Therefore, there is a critical need to identify novel antileukemic drugs with improved chemical properties and efficacy.

Leukemia drug discovery studies have mainly relied on predefined targets identified by genetic abnormalities, differential gene expression, or protein abundance between normal and disease states.[6,7] Traditional target-based drug discovery is then used to identify inhibitors of these targets.[8] However, this process often relies on *in vitro* activity assays, and candidate inhibitors identified using this approach are frequently not cell-permeable, lose their activity, or have unintended consequences within the context of the cell, primarily due to off-target effects.[9] As an alternative approach, chemical genetic drug discovery approaches have utilized cell-based assays to identify anticancer agents, which has been highly successful with adherent cancer cells.[9] However, the difficulty in utilizing

suspension cells for high-throughput chemical screens has hampered the progress in identifying novel inhibitors of bloodborne cancers. Therefore, only a limited number of compounds have been tested for their anticancer activities on human acute myeloid leukemia or lymphoma cells.[10,11] For example, flow-cytometry-based approaches have been used to develop leukemia cell cycle profile responses to compounds.[11] However, these approaches were time-consuming, expensive, and not amenable to high-throughput screening (only capable of processing ∼1000 compounds/day).[11] As an alternative, end point cell viability assays like Alamar Blue staining have been used to identify compounds that inhibit leukemia cell proliferation.[10] However, these approaches lack critical information with regard to the phase of the cell cycle in which these compounds are active that could inform their mechanism of action.[10]

Here, we report the development and application of a novel leukemia suspension cell-based high-throughput chemical screening approach for leukemia cell cycle profiling and antileukemic drug discovery. This approach has practical advantages over previous leukemia drug screening approaches, which include the saving of time and money and compatibility with current screening platforms that are used for adherent cell

chemical screening. This approach is capable of generating a cell cycle profile response for each test compound and allows for easy comparison and ranking of compounds based on leukemia cell responses. Using this approach, we identified novel G1/S-, G2-, and M-phase specific leukemia inhibitors with diverse chemotypes. Importantly, we discovered and characterized the leukemia specific inhibitor 1 (Leusin-1), which specifically arrests leukemia cells during G2 phase and triggers an apoptotic cell death. Leusin-1 showed specificity toward acute lymphoblastic leukemia cells compared to other types of leukemias, nonbloodborne cancers, or normal cells and represents a lead molecule for antileukemic drug development.

■ RESULTS AND DISCUSSION

Discovery of Leukemia Cell Cycle Modulators. The limited efficacy, lack of specificity, and toxic side effects of current antileukemic drugs[2−5] inspired us to establish an integrated high-throughput suspension cell-based strategy for identifying small molecule cell cycle modulators for use in dissecting the mechanisms of leukemia cell proliferation and for the development of novel leukemia therapies (Figure 1A). Briefly, human CCRF-CEM acute lymphoblastic leukemia (ALL) cells were plated into 384-well plates. A diverse compound library (181420 small druglike molecules) encompassing a broad chemical space was used to place one compound per well at a final concentration of 10 μM. The cells were fixed 16 h later and stained with the DNA-selective stain Vybrant DyeCycle Green, which emits a fluorescent signal when exited at 488 nm that is proportional to the DNA mass of a cell. Plates were then scanned with an Acumen eX3 fluorescence microplate cytometer using its 488 nm laser, and a cell cycle histogram profile was generated for each compound (Figure 1A). Cell cycle profiles were ranked according to percent G1/S-phase arrest and percent G2/M-phase arrest (Figure 1B,C and Table S1). An example of a compound from each class and its associated cell cycle profile are shown in panels D and E of Figure 1. Compounds that arrested cells in G1/S phase with >2 standard deviations (SDs) from the dimethyl sulfoxide (DMSO) control or in G2/M phase with >80% of the Taxol control were retested in triplicate to confirm their bioactivity. In total, 30 G1/S-phase and 471 G2/M-phase inhibitors were reconfirmed and accounted for an overall hit rate of 0.28% (Figure 1F and Table S1).

Antileukemic Compound Chemical Analysis. The chemical structures and potential targets of the G1/S-phase and G2/M-phase hit antileukemic compounds were analyzed using CSNAP (Chemical Similarity Network Analysis Pull-down), a recently developed computational compound target inference approach based on chemical similarity networks.[12−15] Specifically, CSNAP compared hit compounds to compounds with annotated targets from the ChEMBL database that shared a high degree of chemical similarity (see Methods for similarity search parameters). The annotated and hit compounds were then ordered into chemical similarity networks where nodes represented compounds and edges represented compound similarities. Using a similarity threshold of 0.6, previously determined to be the optimal threshold for clustering six known drug classes into separate subnetworks from a training compound set,[12] the networks were further partitioned into multiple subnetworks that shared similar chemotypes. The chemical similarity networks were used to predict the targets of query compounds based on a nearest-
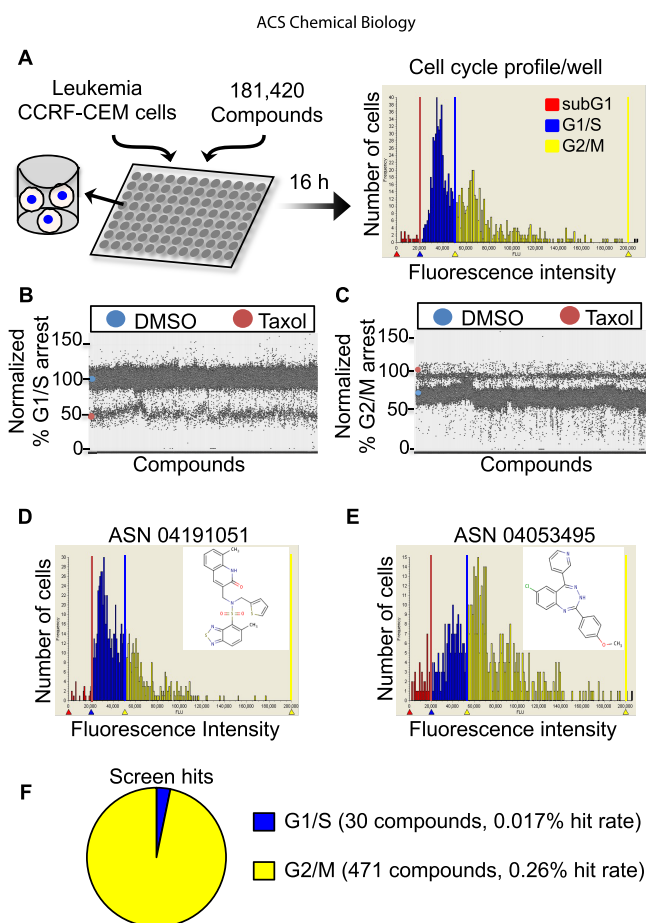
Figure 1. Overview of the leukemia suspension cell-based high-throughput cell cycle profiling chemical screening approach and summary of screening results. (A) Summary of the screening approach in which leukemia CCRF-CEM cells were treated with each of 181420 compounds (at 10 μM) for 16 h. Cells were then fixed and stained with Vybrant DyeCycle Green, and a cytometer was used to generate a cell cycle profile for each compound on the basis of the fluorescence intensity that is proportional to a cell's DNA mass. The fluorescence intensity is in arbitrary units (x-axis), and the total number of cells is on the y-axis. (B and C) Graphs show the percent G1/S-phase and G2/M-phase arrest (y-axis) for each of the 181420 compounds (x-axis). The cutoffs for G1/S-phase inhibitors was set at >2 SDs from the average of the DMSO controls. The cutoff for G2/M-phase inhibitors was set at >80% of the Taxol positive control average. (D and E) Examples of compounds arresting the cell cycle in G1/S phase and G2/M phase and their cell cycle profiles. (F) Summary of screen hits. In total, 30 G1/S-phase inhibitors and 471 G2/M-phase inhibitors were identified with an overall 0.28% hit rate. For panels B−F, see also Table S1.

neighbor scoring function, S-score, that ranks the frequency of targets from annotated compounds in the neighborhood of each query.[16] For our analysis, we generated two chemical similarity networks that corresponded to G1/S- and G2/M-phase networks (Figure 2A,B and Table S2). We visualized the number of predicted targets observed in each cell cycle phase using a heat map in which the color intensity was scaled and normalized according to the S-score of each target (Figure 2C,D and Table S2). Furthermore, we identified the most abundant targets by determining the accumulated S-score ($\sum$S-Score) across both G1/S- and G2/M-phase compounds (Figure 2C,D and Table S2). This analysis grouped the 30 G1/
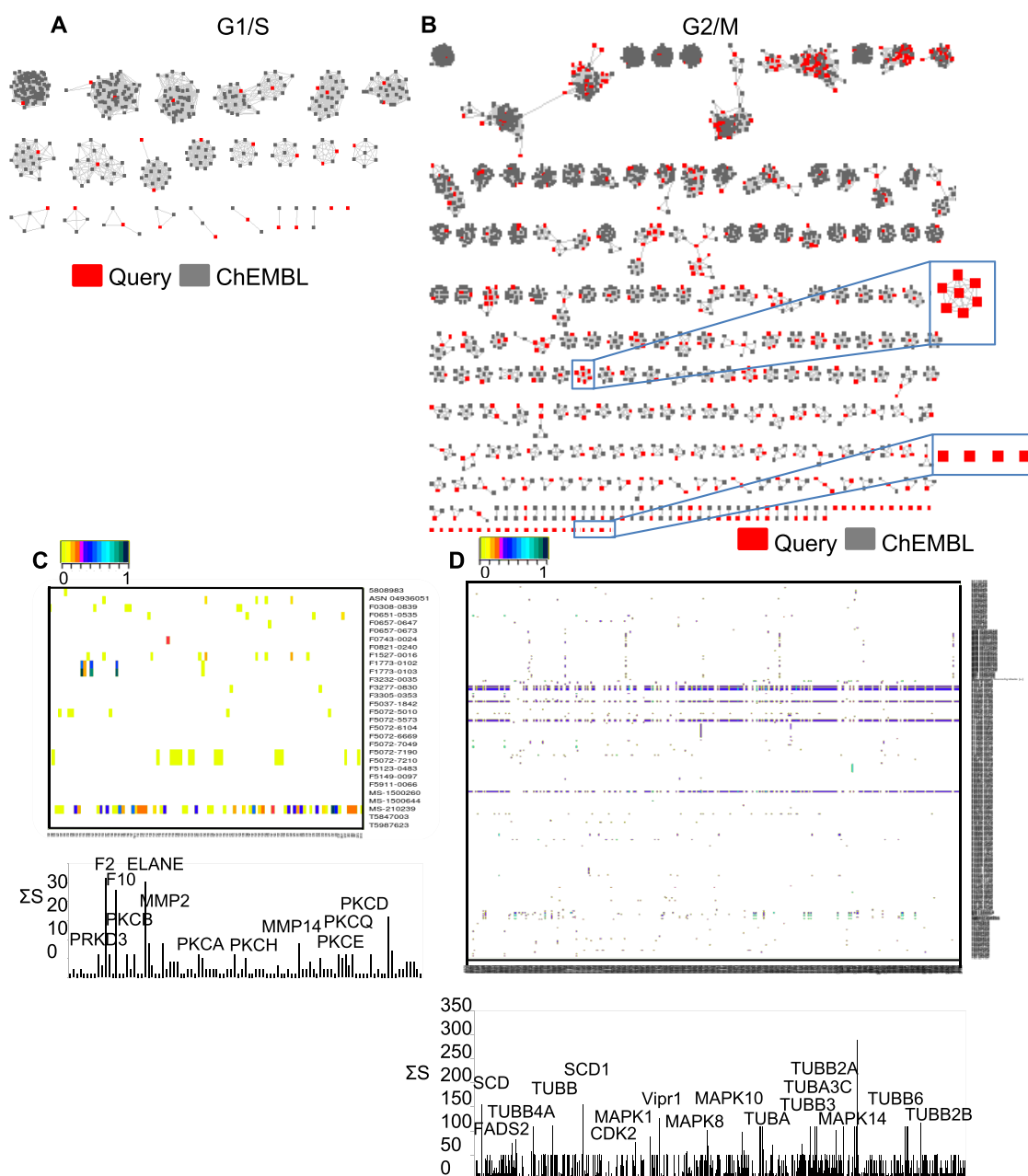
Figure 2. Chemical analysis of leukemia G1/S-phase and G2/M-phase specific inhibitors. (A) CSNAP chemical similarity network of G1/S-phase inhibitors. Note that these compounds are organized into 25 chemotypic clusters and two compounds remained orphaned. Query compounds are colored red, and ChEMBL compounds gray. (B) CSNAP chemical similarity network of G2/M-phase inhibitors. These compounds are organized into 96 chemotypic clusters, and 45 compounds remained orphaned. Query compounds are colored red, and ChEMBL compounds gray. (C and D) Heat map summaries of CSNAP S-scores, scaled from 0 to 1. The cumulative S-score ($\sum S$-score) of each assigned target in the target spectrum and the major predicted targets and off-targets are indicated. For panels A−D, see also Table S2.

S-phase compounds into 25 chemotype clusters and the 471 G2/M-phase compounds into 96 chemotype clusters (Figure 2A,B and Table S2). The top predicted targets for G1/S-phase inhibitors were proteins involved in signaling pathways that promote cell growth and proliferation (Figure 2C and Table S2). The top predicted targets for G2/M-phase inhibitors were tubulin isoforms (Figure 2D and Table S2). Because of our interest in cell division, we sought to analyze the G2/M-phase network further. However, due to the overabundance of screening campaigns aimed at discovering microtubule-targeting agents, we eliminated all chemotype clusters that were predicted to be targeting microtubules (α/β-tubulin)

from further consideration. This resulted in four remaining chemotype clusters and 45 orphan compounds that did not share significant chemical similarity with other compounds in the ChEMBL database (for example, see the boxed compounds in Figure 2B). Two compounds from each novel chemotype cluster and the 45 orphan compounds (total of 53 compounds) were selected, resynthesized, and subjected to further evaluation in secondary assays (Table S3).

G2/M-Phase Antileukemic Compound Potency. To assess the potential of the 53 selected compounds as antileukemic agents, we tested them for their ability to inhibit CCRF-CEM ALL cell viability. For viability assays, cells were
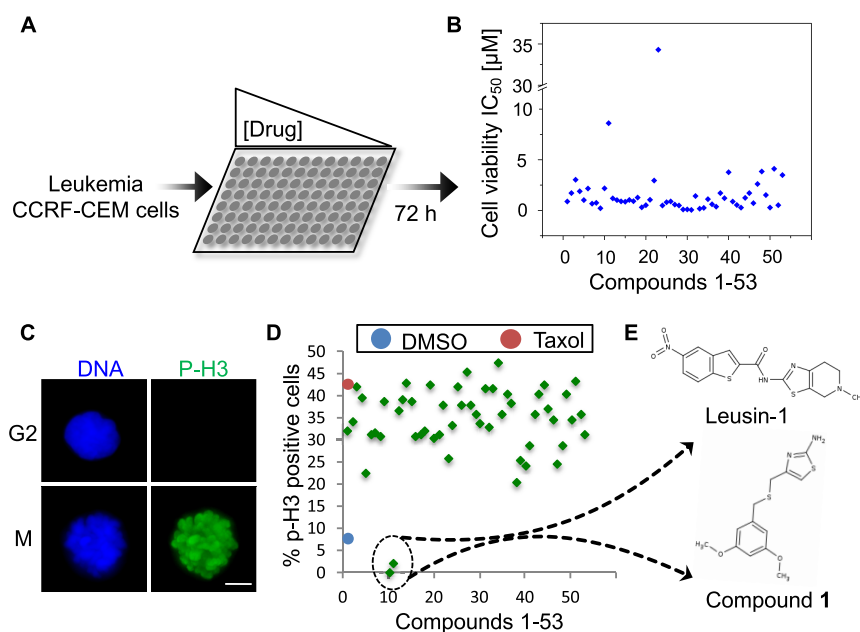
Figure 3. Leukemia G2/M-phase inhibitor potency. (A) CCRF-CEM cells were treated with increasing concentrations (from 95.37 pM to 50 μM) of each compound for 72 h, and the cell viability was assessed using the CellTiter-Glo assay. (B) Summary graph showing the cell viability IC_{50} of each compound (x-axis) on a micromolar scale (y-axis). Note that 53 compounds have an IC_{50} of <5 μM. See also Table S3. (C) Assay for measuring the percentage of mitotic cells. Cells were stained with Hoechst 33342 DNA dye (to measure total cells) and Alexa Fluor 488-pH3 antibodies (to measure the number of mitotic cells). The scale bar indicates 5 μm. (D) Summary of the percentage of cells in mitosis (y-axis) for each of the 53 compounds (x-axis). (E) Chemical structures of Leusin- I and compound **1** G2-phase inhibitors.

treated with each compound for 72 h, and their viability was measured using the CellTiter-Glo luminescent cell viability assay (Promega), which measures total ATP levels (indicative of metabolically active cells) using a luminometer at a wavelength of 560 nm (Figure 3A,B). These assays were carried out in triplicate with a 20-step series of 2-fold dilutions (from 50 μM to 95.37 pM) for each compound, and their cell viabilities, IC_{50} (half-maximal inhibitory concentration), were derived (Figure 3B and Table S3). This analysis revealed that most compounds (51) had an IC_{50} of <5 μM (Figure 3B and Table S3).

Multiparametric Phenotypic Analysis of Leukemia G2/M-Phase Inhibitors. To further explore the mechanism of action of G2/M-phase inhibitors, we analyzed the cellular response of cells to these inhibitors by immunofluorescence (IF) microscopy. Due to the difficulty in performing IF microscopy on CCRF-CEM cells, HeLa cells were treated with each of the 53 compounds at a concentration corresponding to their CCRF-CEM cell viability (IC_{90}) for 16 h. Cells were then fixed, permeabilized, co-stained for DNA and α-tubulin, and imaged at 63× magnification. Surprisingly, 51 compounds arrested cells with depolymerized microtubules, indicating that they represented novel chemotypes that were targeting microtubules (Table S3). Consistently, staining of the cells with a FITC fluorescently labeled antibody that recognizes the mitotic marker phosphorylated histone H3 (p-H3[17,18]) indicated that 51 compounds had an increased percentage of cells arrested in mitosis [% mitotic cells = (number of p-H3 positive cells)/(total number of cells that stained positive with the Hoechst 33342 DNA dye)] compared to controls (Figure 3C,D). However, N-(5-methyl-4,5,6,7-tetrahydrothiazolo[5,4-c]pyridin-2-yl)-5-nitrobenzo[b]thiophene-2-carboxamide hydrochloride [leukemia specific inhibitor 1 (Leusin-1)] and 4-

{[(3,5-dimethoxybenzyl)thio]methyl}thiazol-2-amine (compound **1**) induced a decrease in the percentage of mitotic cells (Figure 3D,E and Table S3). In HeLa cells, Leusin-1 and compound **1** had no effect on the interphase microtubule cytoskeletal network or the mitotic microtubule spindle, even at the high concentration of 137 μM for Leusin-1 or 180 μM for compound **1** (Figure 4A and Figure S1). Further testing of Leusin-1 and compound **1**, using an *in vitro* microtubule polymerization assay, showed that they had no effect on microtubule polymerization, similar to the DMSO control (Figure 4B). In contrast, Taxol increased the rate of microtubule polymerization, whereas colchicine and nocodazole abolished microtubule polymerization (Figure 4B). However, compound **1** proved to be an unstable compound and lost activity over time in suspension. Therefore, we selected Leusin-1 for further analysis on the basis of its novel chemotype, its stable biochemical properties, and its inhibition of leukemia cell division through a G2-phase arresting and non-microtubule targeting mechanism. To further verify that Leusin-1 was a G2-phase inhibitor, we treated CCRF-CEM cells with thymidine (G1/S-phase arrest), Taxol (M-phase arrest), RO-3306 (G2-phase arrest[19]), or Leusin-1 and analyzed the status of cell cycle biochemical markers by immunoblot analysis. Consistently, Taxol, RO-3306, and Leusin-1 arrested cells with lower levels of Cyclin E (levels peak at G1/S phase) and increased levels of Cyclin B (levels peak at G2/M phase) (Figure 4C). However, unlike Taxol, RO-3306 and Leusin-1 also arrested cells with lower levels of p-H3 (present in only M phase) and increased levels of Cyclin A (levels peak in G2 phase) (Figure 4C). Additionally, flow-cytometry analyses of CCRF-CEM cells treated with either DMSO, nocodazole, or Leusin-1 showed that Leusin-1 was arresting cells in G2/M phase (Figure S2). Together, these
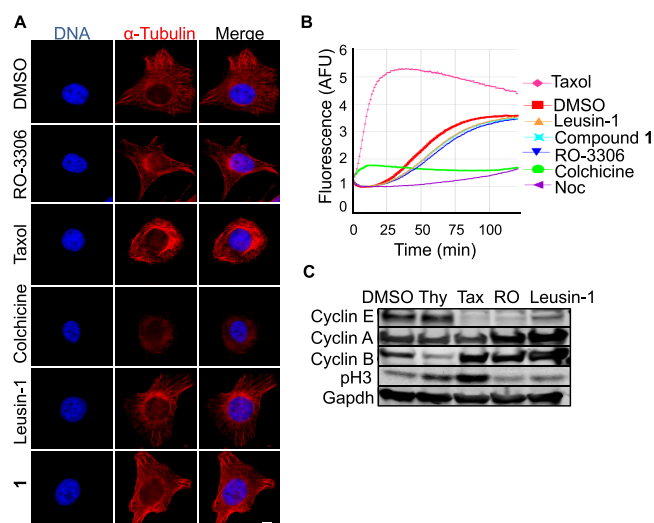
Figure 4. Leusin-1 and compound **1** do not target tubulin. (A) Immunofluorescence microscopy of HeLa cells treated with DMSO, Leusin-1 (137 μM), compound **1** (180 μM), Taxol (100 nM), colchicine (366 nM), or RO-3306 (10 μM) for 3 h and co-stained for α-tubulin (anti-α-tubulin antibodies, red) and DNA (Hoechst 33342, blue). The scale bar indicates 10 μm. For a summary of phenotypic classification for all 53 G2/M-phase inhibitors, see Table S3. (B) Summary of in vitro microtubule polymerization reactions in the presence of DMSO or 3 μM Leusin-1, compound **1**, colchicine, nocodazole, RO-3306, or Taxol. Note that Leusin-1 and compound **1** have no effect on microtubule polymerization. The time is in minutes (x-axis), and AFU denotes arbitrary fluorescence units (y-axis). (C) CCRF-CEM cells were treated with DMSO, thymidine (2 mM), Taxol (100 nM), RO-3306 (10 μM), or Leusin-1 (5 μM) for 24 h. Extracts were prepared and immunoblotted for Cyclin A, B, and E and for the phospho-histone H3 (p-H3 ser10) marker of mitotic cells. Note that Leusin-1-treated cells have low p-H3 and stabilized Cyclin A and B levels, indicative of a failure to enter mitosis, similar to RO-3306. In contrast, Taxol-treated cells arrest in mitosis with high levels of p-H3 and Cyclin A levels are lower.

data indicated that Leusin-1 was arresting CCRF-CEM cells specifically in G2 phase through a nonmicrotubule targeting mechanism.

Leusin-1 Arrests Cells in G2 Phase and Triggers an Apoptotic Cell Death. To determine the consequences of arresting cells in G2 phase with Leusin-1, we analyzed the biochemical response of cells treated with Leusin-1. CCRF-CEM cells were treated with Leusin-1, cisplatin (G2-phase inhibitor), or Taxol (M-phase inhibitor), and protein extracts were prepared after 48 h. Consistent with our previous data, immunoblot analyses of protein samples using antibodies directed against p-H3 (phosphorylated in mitosis) indicated that Leusin-1 and cisplatin arrested cells with limited p-H3 staining, indicative of a G2-phase arrest, whereas Taxol arrested cells with increased p-H3 levels, indicative of a M-phase arrest (Figure 5A). Interestingly, Leusin-1 induced the cleavage of caspase-3, indicative of apoptotic pathway activation (Figure 5A). These data indicated that Leusin-1 arrested cells prior to mitosis and triggered an apoptotic cell death. To further test this, CCRF-CEM cells were treated with DMSO, Leusin-1, or Taxol for 48 h and the extent of caspase-3/7 activation was measured using the Caspase-Glo luminescent caspase activity assay.[20] This assay revealed that Leusin-1 was indeed inducing an apoptotic cell death similar to that seen with Taxol treatment (Figure 5B). Next, we
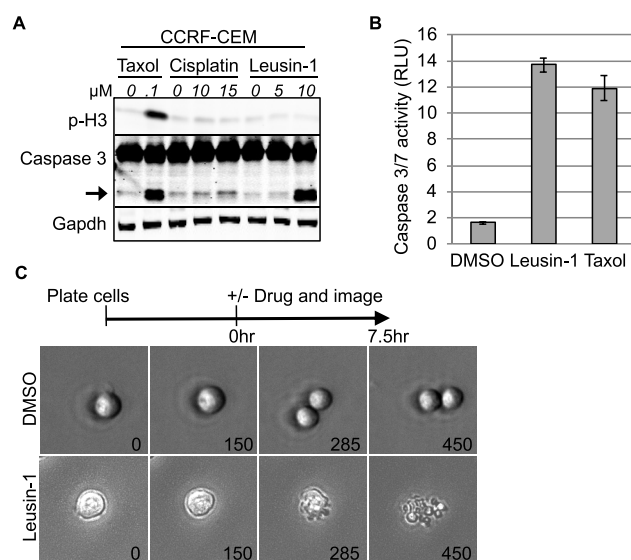
Figure 5. Leusin-1 arrests cells in G2 phase and triggers an apoptotic cell death. (A) CCRF-CEM cells were treated with DMSO or the indicated concentrations of Leusin-1, Taxol, or cisplatin for 48 h. Extracts were prepared and immunoblotted for p-H3, caspase-3, and Gapdh. Note that Leusin-1- and cisplatin-treated cells have low p-H3 levels, indicative of a failure to enter mitosis. In contrast, Taxol-treated cells arrest in mitosis with high levels of p-H3. Also note that Leusin-1 and Taxol treatment led to caspase-3 cleavage (the cleaved product is labeled with an arrow). (B) CCRF-CEM cells were treated with DMSO, Leusin-1 (5 μM), or Taxol (100 nM) for 48 h and the caspase-3/7 activity was quantified using the Caspase-Glo luminescent caspase activity assay. RLU indicates relative light units. Data are presented as the average ± SDs. Note that Leusin-1 induced caspase-3/7 activation, similar to Taxol, indicative of apoptosis. (C) Live-cell time-lapse microscopy of CCRF-CEM cells treated with DMSO or Leusin-1 (5 μM). Note that Leusin-1-treated cells fail to divide and undergo apoptosis.

performed live-cell time-lapse microscopy on CCRF-CEM cells treated with DMSO or Leusin-1. DMSO-treated cells were able to divide normally, whereas Leusin-1-treated cells never divided and eventually underwent apoptosis (Figure 5C and Movies S1 and S2). Together, these data indicated that Leusin-1 was arresting cells in G2 phase and triggering an apoptotic cell death.

Leusin-1 Is an ALL Specific Inhibitor. To determine whether Leusin-1 was active against a broad array of cancers or was specific for leukemias, we treated a diverse panel of cancer cell lines and normal cell lines with Leusin-1 for 72 h. These included cervical adenocarcinoma (HeLa), breast adenocarcinoma (MCF-7), melanoma (M233), osteosarcoma (U-2 OS), lung adenocarcinoma (NCI-H560), acute lymphoblastic leukemia (CCRF-CEM), retinal pigment epithelial (hTERT-RPE), lymphoma (Jeko-1), and colorectal carcinoma (HCT 116) cells. Cell viability IC_{50} was then quantified and compared to that of the DMSO control (Figure 6A). Interestingly, Leusin-1 showed specificity for CCRF-CEM cells compared to all other adherent types of cancers (CCRF-CEM cell viability IC_{50} for Leusin-1 = 2.64 μM compared to values 4−50-fold higher for all other cell lines) (Figure 6A). To determine if Leusin-1 was active against all leukemias (non-adherent cells) or only a subset of leukemias, we analyzed the efficacy of Leusin-1 on a panel of leukemia cell lines. These included acute lymphoblastic leukemia (ALL; CCRF-CEM
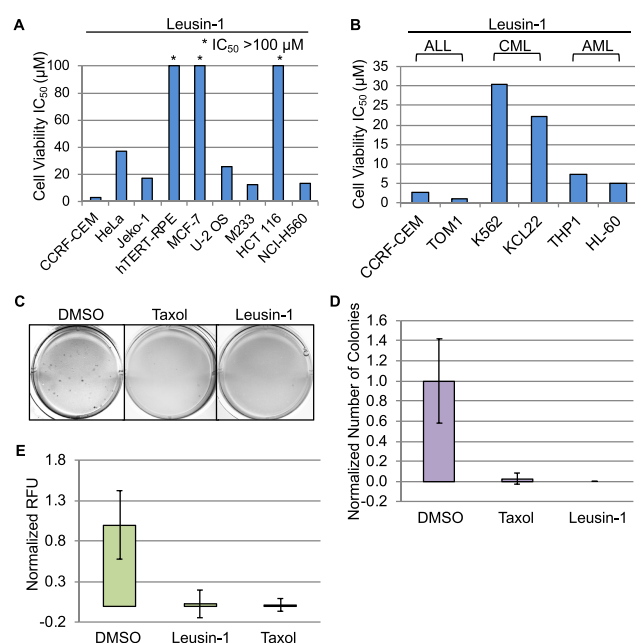
Figure 6. Leusin-1 inhibits ALL proliferation. (A) A broad panel of cancer cell lines was treated with increasing concentrations of Leusin-1 for 72 h, and their cell viability IC_{50} was assessed using the CellTiter-Glo assay. The graph shows the summary of results for cell viability IC_{50} (y-axis) for each cell line (x-axis). (B) A panel of leukemia cells were treated with increasing concentrations of Leusin-1, and cell viability IC_{50} (y-axis) was determined for each cell line (x-axis): ALL (CCRF-CEM and TOM1), AML (HL-60 and THP1), and CML (K562 and KCL22). (C and D) ALL clonogenic assay. ALL CCRF-CEM cells were treated with DMSO, Leusin-1 (2 μM), or Taxol (50 nM) for 3 weeks, and the percent colony formation, normalized to DMSO, was quantified. Data are represented as the average percent ± SDs. (E) ALL transformation assay. ALL CCRF-CEM cells were treated with DMSO, Leusin-1 (2 μM), or Taxol (50 nM) for 7 days, and the total fluorescence was quantified. Data are represented as the average percent ± SDs.

and TOM1), acute myeloid leukemia (AML; HL-60 and THP1), and chronic myeloid leukemia (CML; K562 and KCL22) cell lines. Surprisingly, ALL cell lines were the most sensitive to Leusin-1 (CCRF-CEM IC_{50} = 2.66 μM and TOM1 IC_{50} = 0.877 μM, compared to values of 5−30 μM for all other leukemia cell lines) (Figure 6B). These results indicated that Leusin-1 was most potent against acute lymphoblastic leukemias.

Leusin-1 Inhibits ALL Colony Formation. Next, we assessed the ability of Leusin-1 to inhibit CCRF-CEM colony formation using two separate clonogenic assays (Figure 6C−E). First, an agar-based colony formation assay was performed in the presence of DMSO, Taxol, or Leusin-1; colony formation was visualized with crystal violet stain, and the total number of colonies was quantified. Interestingly, Leusin-1 was able to inhibit colony formation like Taxol (Figure 6C,D). Next, we analyzed the effect of Leusin-1 on colony formation using the CytoSelect Cell Transformation Assay kit (Cell Biolabs, Inc.), which measures the total number of viable cells in agar solutions. Consistently, Leusin-1 inhibited colony formation like Taxol (Figure 6E). Together, these data indicated that Leusin-1 was inhibiting CCRF-CEM colony formation.

Conclusions. Cell cycle checkpoints ensure that the progression of the cell cycle from one phase to another is regulated with precision and occurs with high fidelity.[21] Dysregulation of the G1/S-, S-, G2-, and M-phase cell cycle checkpoints can lead to abnormal cell proliferation and carcinogenesis.[21] A strategy for developing leukemia therapeutics has been to develop inhibitors that perturbed the cell cycle and lead to a cell cycle arrest and subsequent apoptotic cell death.[22,23] However, the difficulty of analyzing the cell cycle response of suspension cells to chemical treatments has hampered leukemia cell-based high-throughput drug discovery efforts. Although a limited number of compounds have been screened in acute myeloid leukemia and lymphoma cells, these studies have relied on flow cytometry that is not easily amenable to high-throughput screening or on end point assays that lack critical information about the cell cycle phase where these compounds are active.[10,11] To address this, we engineered our high-throughput cell cycle profiling chemical screening platform to be compatible with suspension leukemia cells and screened 181420 druglike compounds in leukemia CCRF-CEM cells.[14] Importantly, this approach bypasses the need for flow cytometry and makes use of a laser scanning cytometer that is a staple of modern screening platforms. The use of laser scanning cytometery has the added benefits of reducing screening costs and screening run time while increasing throughput and the impact of data analyses. In comparison to end point chemical screens that use cell viability to select hit compounds, this approach provides a cell cycle profile for each drug that not only provides information about cell viability (cell death is represented by the subG1 population of cells) but also provides critical information about the cell cycle phase in which the drug is active. This additional cell cycle chemical profiling information can be used to better focus downstream experimentation to define the drug mechanism of action. Additionally, when coupled with chemical similarity analyses, like CSNAP, the cell cycle profile can be used to validate drug target predictions. For example, a hit drug predicted to be an analogue of Taxol (a known M-phase inhibitor) would be expected to have a cell cycle profile with an increased percentage of cells in M phase. Thus, this approach has several advantages that should help expedite leukemia drug discovery and characterization.

Our leukemia cell cycle chemical profiling approach yielded novel G1/S-, G2-, and M-phase specific inhibitors of acute lymphoblastic leukemia cell proliferation, which included novel chemotypes that were targeting each cell cycle phase. Although we did not pursue the M-phase microtubule-targeting agents, it is important to note that microtubule-targeting agents continue to be used broadly for the treatment of cancer and the new chemotypes discovered in this study could be used to develop more effective microtubule-targeting therapeutics.[24] Our data indicate that Leusin-1 is an exciting molecule to pursue for developing new acute lymphoblastic leukemia therapies. First, Leusin-1 potently arrests the leukemia cell cycle in G2 phase and triggers an apoptotic cell death, thereby inhibiting leukemia cell proliferation. Second, Leusin-1 is not a microtubule-targeting agent, which is often associated with numerous side effects like neurotoxicities and neutropenia.[24] Third, in comparison to other leukemia therapeutics, either in the clinic or approved for the treatment of leukemias like vinblastine by the Food and Drug Administration, Leusin-1 appears to have a greater specificity for leukemia cells (ALL in particular) compared to other cancer cell types and normal cells. This Leusin-1 specificity for acute lymphoblastic leukemias represents a vantage point for the development of

therapeutics with a more favorable therapeutic window. Future studies related to defining the Leusin-1 mechanism of action should help to elucidate the underlying sensitivity of acute lymphoblastic leukemias to Leusin-1.

■ METHODS

Compounds. Leusin-1 and compound **1** were purchased from Life Chemicals Inc. at >95% purity. For ^{1}H NMR of Leusin-1 and compound **1**, see Figure S3.

Cell Culture. All human cell lines, with the exception of M233, were purchased from ATCC. Their identities were verified by short-tandem repeat profiling. Cells were passaged for <6 months following receipt and were maintained in 5% CO_2 at 37 °C in RPMI 1640 medium (CCRF-CEM, Jeko-1, NCI-H560, TOM1, KCL22, and THP1), DMEM/F12 (HeLa and hTERT-RPE), McCoy's 5A (U-2 OS and HCT 166), IMDM (K562 and HL-60), or EMEM (MCF-7) with 10% fetal bovine serum (FBS), 2 mM L-glutamine, and antibiotics. M233 was established from a patient biopsy under UCLA IRB Approval 02-08-067, as described previously.[25] M233 was genotyped using the Oncomap3 platform for 33 genes, Affymetrix Gene Chip for SNP, and Ion Torrent for next-generation sequencing, passaged for <6 months following verification, and maintained in RPMI 1640 medium with 10% FBS and antibiotics in 5% CO_2 at 37 °C. All media were purchased from ThermoFisher.

High-Throughput Screening. Screening conditions were as described previously,[14] with the following modifications. CCRF-CEM cells were plated in 384-well plates (1000 cells/well) and treated with 10 μM drugs for 16 h. Cells were fixed with 4% paraformaldehyde and stained with 2.5 μM Vybrant DyeCycle Green (Invitrogen) for 3 h at room temperature. Plates were scanned with an Acumen eX3 (TTP Labtech) fluorescence cytometer using its 488 nm laser, and a cell cycle histogram profile was generated for each well. For the G2/M-phase secondary screen, 16 h after the addition of the drug HeLa cells were fixed with 4% paraformaldehyde, permeabilized with 0.1% Triton X-100/phosphate-buffered saline (PBS), and stained with Alexa Fluor 488 phospho-histone-H3 (Ser10, Cell Signaling) and 0.25 μg/mL Hoechst 33342 for 1 h. Plates were washed twice with PBS using a microplate washer (BioTek) and then imaged with an ImageXpress Micro (Molecular Devices) high-content fluorescence microscope. Data analysis was performed using the CDD (Collaborative Drug Discovery) software, and outputs were exported to Excel.

Compound Potency. For cell viability IC_{50}, CCRF-CEM cells were treated with a 20-step series of 2-fold dilutions (from 50 μM to 95.37 pM). Cell viability IC_{50} was determined using the CellTiter-Glo Assay (Promega), which measures total ATP levels. Plates were read with a Tecan M1000 microplate reader at 540 nm, and CDD software was used for generating IC_{50} and IC_{90} values.

Immunofluorescence and Time-Lapse Microscopy. Immunofluorescence microscopy was carried out as described previously[26] using HeLa cells, except that images were captured with a Leica DMI6000 microscope (Leica Microsystems) and deconvolved with Leica deconvolution software. Time-lapse microscopy was performed as described previously.[17] Briefly, CCRF-CEM cells were treated with DMSO or Leusin-1 (5 μM), and 10 Z-stack images (0.9 μm steps) were captured at 15 min intervals. Images were deconvolved and converted to AVI movie files.

Apoptosis Assays. CCRF-CEM cells were treated with the indicated drugs for 48 h, and the Caspase-Glo luminescent caspase activity assay (Promega) was used to measure the activity of effector caspases, as a readout of apoptosis. Plates were scanned with a luminometer at a wavelength of 520 nm, and the apoptotic index [(total caspase activity)/(total number of cells)] per well was measured. Quantitation is in relative light units (RLU) compared to the DMSO control.

Leukemia Clonogenic Assays. Five thousand CCRF-CEM cells per well were grown in six-well plates with semisolid RPMI 1640 medium containing 10% FBS, 0.45% agarose, and drug (1% DMSO, 2 μM Leusin-1, or 50 nM Taxol). A layer of 500 μL of medium containing the corresponding drug was added on top, and plates were

incubated in 5% CO_2 at 37 °C for 3 weeks. Fresh medium was replenished twice a week. Colonies (>30 cells) were scored and visualized after the addition of 0.005% crystal violet overnight.

Leukemia Cell Transformation Assay. The CytoSelect 96 Well Cell Transformation Assay kit (Cell Biolabs, Inc.) was used for assessing soft agar colony formation following the manufacturer's instructions for 7 days. Fluorescent signals from cells treated with DMSO, Leusin-1 (2 μM), or Taxol (50 nM) were normalized after subtracting the value from the no cell blank, and the mean values of the samples were plotted as relative light units (RLU).

CSNAP Chemical Analysis. CSNAP was used to predict the targets of G1/S-phase and G2/M-phase inhibitors as described previously.[12] Briefly, compounds were queried in annotated ChEMBL database version 18 using the following search parameters: Tanimoto cutoff of 0.75 and z-score cutoff of 2.5. The ChEMBL target annotations were retrieved from the database on the basis of the following criteria: confidence score of 4 and binding assay type. Finally, chemical similarity networks and ligand−target interaction fingerprints (LTIFs) were analyzed using Cytoscape and the R statistical package, respectively.

***In Vitro* Tubulin Polymerization Assays.** Tubulin polymerization reactions were carried out according to the manufacturer's instructions (Cytoskeleton, BK011P) in the presence of DMSO and 3 μM Leusin-1, compound **1**, Taxol, or colchicine. Polymerization was monitored with a Tecan M1000 microplate reader at 420 nm for 120 min at 37 °C.

Antibodies. The following antibodies were used in this study: phospho-histone-H3 Alexa Fluor 488 (Ser10) (Cell Signaling, catalog no. 3465); α-tubulin (Serotec, catalog no. MCAP77G); caspase-3 (Cell Signaling Technology, catalog no. 9665); p-H3 (Cell Signaling, catalog no. 9701); Cyclin A, Cyclin B, and Cyclin E (Santa Cruz Biotechnology, catalog nos. sc-751, sc-245, and sc-481, respectively); and Gapdh (GeneTex, catalog no. GTX627408). FITC- and Cy3-conjugated secondary antibodies were from Jackson Immuno Research.

Software. The CSNAP program is available as a web server http://services.mbi.ucla.edu/CSNAP/.

Statistical Analysis. The quality of the screen was assessed by calculating the Z' factor [Z' factor = $1 − 3(\sigma_p + \sigma_n)/(|\mu_p − \mu_n|)$], which takes into account the dynamic range of the assay and the variance of the data.[27] The screen was performed with an average plate Z' factor of 0.48 ± 0.06, close to the optimal performance range of 0.5−1.[27]

■ ASSOCIATED CONTENT

Ⓢ Supporting Information

The Supporting Information is available free of charge on the ACS Publications website at DOI: 10.1021/acschembio.9b00173.

Figures S1−S3, including ^{1}H NMR spectra for Leusin-1 and compound **1**, and descriptions of Tables S1−S3 and Movies S1 and S2 (PDF)

Table S1 (XLSX)

Table S2 (XLS)

Table S3 (XLS)

Movie S1 (MOV)

Movie S2 (MOV)

■ AUTHOR INFORMATION

Corresponding Author

*Department of Chemistry and Biochemistry, UCLA, Los Angeles, CA 90095. Phone: 310-206-2092. E-mail: torres@chem.ucla.edu.

ORCID Ⓘ

Jorge Z. Torres: 0000-0002-2158-889X

Author Contributions

X.X. and J.Z.T. initiated the project, designed experiments, and analyzed results with input from all authors. A.A.G., S.S., J.Y.O., and E.F.V. performed biochemical and cellular assays. Y.-C.L. performed CSNAP chemical analyses. R.D. provided compound procurement and compound structure preparation.

Notes

The authors declare no competing financial interest.

■ REFERENCES

(1) Pui, C. H., and Jeha, S. (2007) New therapeutic strategies for the treatment of acute lymphoblastic leukaemia. *Nat. Rev. Drug Discovery 6*, 149−165.

(2) Vagace, J. M., De la Maya, M. D., Caceres-Marzal, C., Gonzalez de Murillo, S., and Gervasini, G. (2012) Central nervous system chemotoxicity during treatment of pediatric acute lymphoblastic leukemia/lymphoma. *Critical Reviews in Oncology/Hematology 84*, 274.

(3) Shaffer, B. C., Gillet, J. P., Patel, C., Baer, M. R., Bates, S. E., and Gottesman, M. M. (2012) Drug resistance: Still a daunting challenge to the successful treatment of AML. *Drug Resist. Updates 15*, 62−69.

(4) Woessner, D. W., Lim, C. S., and Deininger, M. W. (2011) Development of an effective therapy for chronic myelogenous leukemia. *Cancer J. 17*, 477−486.

(5) Wierda, W. G., Chiorazzi, N., Dearden, C., Brown, J. R., Montserrat, E., Shpall, E., Stilgenbauer, S., Muneer, S., and Grever, M. (2010) Chronic lymphocytic leukemia: new concepts for future therapy. *Clin Lymphoma Myeloma Leuk 10*, 369−378.

(6) Iacobucci, I., Papayannidis, C., Lonetti, A., Ferrari, A., Baccarani, M., and Martinelli, G. (2012) Cytogenetic and molecular predictors of outcome in acute lymphocytic leukemia: recent developments. *Curr. Hematol Malig Rep 7*, 133−143.

(7) Kristensen, V. N., Lingjaerde, O. C., Russnes, H. G., Vollan, H. K., Frigessi, A., and Borresen-Dale, A. L. (2014) Principles and methods of integrative genomic analyses in cancer. *Nat. Rev. Cancer 14*, 299−313.

(8) Martell, R. E., Brooks, D. G., Wang, Y., and Wilcoxen, K. (2013) Discovery of novel drugs for promising targets. *Clin. Ther. 35*, 1271−1281.

(9) Cong, F., Cheung, A. K., and Huang, S. M. (2012) Chemical genetics-based target identification in drug discovery. *Annu. Rev. Pharmacol. Toxicol. 52*, 57−78.

(10) McDermott, S. P., Eppert, K., Notta, F., Isaac, M., Datti, A., Al-Awar, R., Wrana, J., Minden, M. D., and Dick, J. E. (2012) A small molecule screening strategy with validation on human leukemia stem cells uncovers the therapeutic efficacy of kinetin riboside. *Blood 119*, 1200−1207.

(11) Gasparetto, M., Gentry, T., Sebti, S., O'Bryan, E., Nimmanapalli, R., Blaskovich, M. A., Bhalla, K., Rizzieri, D., Haaland, P., Dunne, J., and Smith, C. (2004) Identification of compounds that enhance the anti-lymphoma activity of rituximab using flow cytometric high-content screening. *J. Immunol. Methods 292*, 59−71.

(12) Lo, Y. C., Senese, S., Li, C. M., Hu, Q., Huang, Y., Damoiseaux, R., and Torres, J. Z. (2015) Large-scale chemical similarity networks for target profiling of compounds identified in cell-based chemical screens. *PLoS Comput. Biol. 11*, e1004153.

(13) Lo, Y. C., Senese, S., Damoiseaux, R., and Torres, J. Z. (2016) 3D Chemical Similarity Networks for Structure-Based Target Prediction and Scaffold Hopping. *ACS Chem. Biol. 11*, 2244−2253.

(14) Senese, S., Lo, Y. C., Huang, D., Zangle, T. A., Gholkar, A. A., Robert, L., Homet, B., Ribas, A., Summers, M. K., Teitell, M. A., Damoiseaux, R., and Torres, J. Z. (2014) Chemical dissection of the cell cycle: probes for cell biology and anti-cancer drug development. *Cell Death Dis. 5*, e1462.

(15) Lo, Y. C., Senese, S., France, B., Gholkar, A. A., Damoiseaux, R., and Torres, J. Z. (2017) Computational Cell Cycle Profiling of Cancer Cells for Prioritizing FDA-Approved Drugs with Repurposing Potential. *Sci. Rep. 7*, 11261.

(16) Lo, Y. C., Rensi, S. E., Torng, W., and Altman, R. B. (2018) Machine learning in chemoinformatics and drug discovery. *Drug Discovery Today 23*, 1538−1546.

(17) Torres, J. Z., Summers, M. K., Peterson, D., Brauer, M. J., Lee, J., Senese, S., Gholkar, A. A., Lo, Y. C., Lei, X., Jung, K., Anderson, D. C., Davis, D. P., Belmont, L., and Jackson, P. K. (2011) The STARD9/Kif16a Kinesin Associates with Mitotic Microtubules and Regulates Spindle Pole Assembly. *Cell 147*, 1309−1323.

(18) Hendzel, M. J., Wei, Y., Mancini, M. A., Van Hooser, A., Ranalli, T., Brinkley, B. R., Bazett-Jones, D. P., and Allis, C. D. (1997) Mitosis-specific phosphorylation of histone H3 initiates primarily within pericentromeric heterochromatin during G2 and spreads in an ordered fashion coincident with mitotic chromosome condensation. *Chromosoma 106*, 348−360.

(19) Vassilev, L. T., Tovar, C., Chen, S., Knezevic, D., Zhao, X., Sun, H., Heimbrook, D. C., and Chen, L. (2006) Selective small-molecule inhibitor reveals critical mitotic functions of human CDK1. *Proc. Natl. Acad. Sci. U. S. A. 103*, 10660−10665.

(20) Chowdhury, I., Tharakan, B., and Bhat, G. K. (2008) Caspases - an update. *Comp. Biochem. Physiol., Part B: Biochem. Mol. Biol. 151*, 10−27.

(21) Williams, G. H., and Stoeber, K. (2012) The cell cycle and cancer. *J. Pathol 226*, 352−364.

(22) Halicka, H. D., Seiter, K., Feldman, E. J., Traganos, F., Mittelman, A., Ahmed, T., and Darzynkiewicz, Z. (1997) Cell cycle specificity of apoptosis during treatment of leukaemias. *Apoptosis 2*, 25−39.

(23) Ghelli Luserna di Rora', A., Iacobucci, I., and Martinelli, G. (2017) The cell cycle checkpoint inhibitors in the treatment of leukemias. *J. Hematol. Oncol. 10*, 77.

(24) Arnst, K. E., Banerjee, S., Chen, H., Deng, S., Hwang, D. J., Li, W., and Miller, D. D. (2019) Current advances of tubulin inhibitors as dual acting small molecules for cancer therapy. *Med. Res. Rev.*, DOI: 10.1002/med.21568.

(25) Sondergaard, J. N., Nazarian, R., Wang, Q., Guo, D., Hsueh, T., Mok, S., Sazegar, H., MacConaill, L. E., Barretina, J. G., Kehoe, S. M., Attar, N., Von Euw, E., Zuckerman, J. E., Chmielowski, B., Comin-Anduix, B., Koya, R. C., Mischel, P. S., Lo, R. S., and Ribas, A. (2010) Differential sensitivity of melanoma cell lines with BRAFV600E mutation to the specific Raf inhibitor PLX4032. *J. Transl. Med. 8*, 39.

(26) Torres, J. Z., Ban, K. H., and Jackson, P. K. (2010) A Specific Form of Phospho Protein Phosphatase 2 Regulates Anaphase-promoting Complex/Cyclosome Association with Spindle Poles. *Mol. Biol. Cell 21*, 897−904.

(27) Zhang, J. H., Chung, T. D., and Oldenburg, K. R. (1999) A Simple Statistical Parameter for Use in Evaluation and Validation of High Throughput Screening Assays. *J. Biomol. Screening 4*, 67−73.